

# Elucidating Metabolic Maturation in the Healthy Fetal Brain Using $^1\text{H}$ -MR Spectroscopy

I.E. Evangelou, A.J. du Plessis, G. Vezina, R. Noeske, and C. Limperopoulos



## ABSTRACT

**BACKGROUND AND PURPOSE:**  $^1\text{H}$ -MRS provides a noninvasive way to study fetal brain maturation at the biochemical level. The purpose of this study was to characterize in vivo metabolic maturation in the healthy fetal brain during the second and third trimester using  $^1\text{H}$ -MRS.

**MATERIALS AND METHODS:** Healthy pregnant volunteers between 18 and 40 weeks gestational age underwent single voxel  $^1\text{H}$ -MRS. MR spectra were retrospectively corrected for motion-induced artifacts and quantified using LCModel. Linear regression was used to examine the relationship between absolute metabolite concentrations and ratios of total NAA, Cr, and Cho to total Cho and total Cr and gestational age.

**RESULTS:** Two hundred four spectra were acquired from 129 pregnant women at mean gestational age of  $30.63 \pm 6$  weeks. Total Cho remained relatively stable across the gestational age ( $r^2 = 0.04, P = .01$ ). Both total Cr ( $r^2 = 0.60, P < .0001$ ) as well as total NAA and total NAA to total Cho ( $r^2 = 0.58, P < .0001$ ) increased significantly between 18 and 40 weeks, whereas total NAA to total Cr exhibited a slower increase ( $r^2 = 0.12, P < .0001$ ). Total Cr to total Cho also increased ( $r^2 = 0.53, P < .0001$ ), whereas total Cho to total Cr decreased ( $r^2 = 0.52, P < .0001$ ) with gestational age. The cohort was also stratified into those that underwent MRS in the second and third trimesters and analyzed separately.

**CONCLUSIONS:** We characterized metabolic changes in the normal fetal brain during the second and third trimesters of pregnancy and derived normative metabolic indices. These reference values can be used to study metabolic maturation of the fetal brain in vivo.

**ABBREVIATIONS:** GA = gestational age; tCho = total Cho (glycerol 3-phosphocholine + phosphocholine); tCr = total Cr (phosphocreatine + Cr); tNAA = total NAA (NAA + *N*-acetyl aspartylglutamate)

$^1\text{H}$ -MR spectroscopy provides a noninvasive method to study brain maturation at the biochemical level. Early metabolic changes observed by  $^1\text{H}$ -MRS may precede morphologic brain changes<sup>1</sup> and overt clinical signs of disease,<sup>2</sup> which makes it an invaluable tool for providing insights into the mechanisms of

brain insult and antecedents of injury. The spectra obtained by  $^1\text{H}$ -MRS depict several metabolites dominated by a large water resonance. When this water signal is suppressed, the metabolites emerge at different resonant frequencies and are expressed as parts per million. Each metabolite reflects specific cellular and biochemical processes. *N*-acetylaspartate is considered a neuronal-axonal marker with a neuronal bioenergetic role<sup>3-5</sup> found in the brain and spinal cord, creatine is involved in energy metabolism through the Cr kinase reaction generating phosphocreatine, and, in turn, adenosine triphosphate,<sup>6</sup> and choline containing compounds of glycerol 3-phosphocholine and phosphocholine which is present at high levels in glial cells<sup>7</sup> as intermediaries in the synthesis of acetylcholine.<sup>8</sup> Lactate, a by-product of anaerobic metabolism, is not normally present but may be detectable by  $^1\text{H}$ -MRS in certain pathologies.<sup>9-11</sup>

The application of  $^1\text{H}$ -MRS in studying the fetal brain in vivo has been explored since the 1990s,<sup>12</sup> and a number of reviews have been published.<sup>13-15</sup> However, there is a paucity of standardized  $^1\text{H}$ -MRS measurements and reference values for fetal brain metabolites from normal healthy pregnancies. Small sample sizes

Received April 27, 2015; accepted after revision June 21.

From the Divisions of Diagnostic Imaging and Radiology (I.E.E., G.V., C.L.) and Fetal and Transitional Medicine (A.J.D.P., C.L.), Children's National Medical Center, Washington, DC; Departments of Pediatrics (I.E.E., A.J.D.P., G.V., C.L.) and Radiology (I.E.E., G.V.), The George Washington University School of Medicine and Health Sciences, Washington, DC; and Applied Science Laboratory, GE Healthcare, Berlin, Germany (R.N.).

This study was funded by the Canadian Institutes of Health Research: MOP-81116 (C. Limperopoulos).

Paper previously presented in part at: Annual Meeting of the Pediatric Academic Societies, May 4-7, 2013; Washington, DC.

Please address correspondence to Catherine Limperopoulos, PhD, Diagnostic Imaging and Radiology/Fetal and Transitional Medicine, Children's National Medical Center, 111 Michigan Ave NW, Washington, DC 20010; e-mail: climpero@childrensnational.org

Indicates open access to non-subscribers at www.ajnr.org

<http://dx.doi.org/10.3174/ajnr.A4512>

have also limited the wide application and diagnostic value of this approach in the fetus. The purpose of this article was to characterize prospectively the trajectory of in vivo metabolic brain maturation of the healthy fetus in the second and third trimesters, and to provide reliable reference values for the interpretation of single voxel  $^1\text{H}$ -MRS of the fetal brain.

## MATERIALS AND METHODS

### Subjects

This Health Insurance Portability and Accountability Act compliant prospective study was approved by the institutional review board of Children's National Medical Center, and written informed consent was obtained by all the study participants. Healthy volunteers between 18 and 40 weeks of pregnancy were consecutively recruited from 2011 through 2014 in low-risk obstetric clinics. In 2012, the protocol was amended to include serial studies of the same subject. Inclusion criteria were normal fetal sonography studies and the absence of any maternal medical conditions that might interfere with normal fetal growth and development (eg, chronic hypertension, preeclampsia, intrauterine growth restriction, placental abnormalities, gestational diabetes, and a known history of congenital heart disease).<sup>16,17</sup> Those with multiple gestations, evidence of congenital infection, documented prenatal chromosomal abnormalities, fetal sonography findings of dysmorphic features, dysgenetic brain lesions, or anomalies of other organ systems, and any maternal contraindication to MR (eg, mechanical heart valve, pacemaker, or any other ferromagnetic implants) were also excluded. No maternal or fetal sedation was used during the MR studies. Retrospectively, those with incidental findings or abnormalities documented in the MR imaging report by the pediatric neuroradiologist (G.V.) were also excluded from the study cohort.

### MR Imaging and Spectroscopy Acquisition

MR imaging and single voxel  $^1\text{H}$ -MRS data for all the subjects were acquired on a 1.5T MR scanner (Discovery MR450; GE Healthcare, Milwaukee, Wisconsin) using an 8-channel surface coil (GE Healthcare) as part of a comprehensive MR imaging protocol. Anatomic single-shot FSE T2WI with TR = 1100 milliseconds and TE = 160 milliseconds, field of view  $320 \times 320 \text{ mm}^2$ , 2-mm section thickness, and 40–60 sections for total brain coverage was acquired in all 3 orthogonal planes. The MR images were reviewed by a neuroradiologist to exclude structural brain abnormality. A single-voxel point-resolved spectroscopy sequence with chemical shift selective suppression was used with TR = 1500 milliseconds; TE = 144 milliseconds; 128–192 excitations that contained 2048 complex points that covered a spectral bandwidth of 2500 Hz, with the phase of all 3 radiofrequency excitation pulses alternating from  $0^\circ$  to  $180^\circ$ ; 16 nonwater-suppressed excitations as reference data; and 6 outer volume suppression pulses around an isotropic voxel, either  $25 \times 25 \times 25$  or  $30 \times 30 \times 30 \text{ mm}^3$ , depending on gestational age (GA) and brain size, with an acquisition time of 3:48 or 5:24 minutes, respectively. The voxel was placed in the middle of the brain posterior to the basal ganglia, encompassing the thalamus and hypothalamus, while avoiding the scalp and extracranial tissues and preventing contamination of the spectra by unwanted lipid signals (Fig 1), using

the anatomic T2WI for guidance. Automatic prescanning and shimming procedures were performed, followed by fine adjustment of the center frequency, transmitter and receiver gains, and linear shims. Before the spectra acquisition, the water suppression level was verified to be  $>95\%$ , and the line width at full width at half maximum to be  $\leq 4 \text{ Hz}$ , which indicated good quality shimming and high spectral resolution for water suppression to accurately resolve the adjacent Cho and Cr peaks at 3.19 ppm and 3.02 ppm, respectively. Mean transmit and receive gains (R1, R2) were  $166 \pm 6$ ,  $13 \pm 1$  and  $29 \pm 2$ , respectively, for all acquired spectra. During the course of the study, the stability and drift of the MR scanner center frequency, transmit gains, and receive gains (R1, R2) were monitored weekly with quality assurance scans of the "Braino" MR spectroscopy sphere phantom (GE Healthcare) using the single-voxel point-resolved spectroscopy sequence.

### MR Spectroscopy Processing

Raw spectra as P-files were transferred to an off-line Linux workstation (The Linux Foundation, San Francisco, California) for correction of motion-induced artifacts due to fetal movement and maternal breathing during acquisition using a retrospective methodology described previously.<sup>18</sup> Resulting spectra were then fitted to basis spectra using the LCModel software (<http://www.lcmodel.com/>)<sup>19</sup> (to calculate metabolite concentrations in the chemical shift range of 4.0–1.0 ppm using the unsuppressed water signal as the internal reference).<sup>20</sup> The MR visible water concentration<sup>21</sup> in the voxel was calculated to be 50,013 mmol/L using the mean water content in the ex vivo cerebrum as  $901 \pm 11.48 \text{ g/M}$ , in the range of 18–40 weeks of gestation,<sup>22</sup> and the molar mass of water, which is approximately 18.02 g/M.<sup>23</sup> This was set in the LCModel parameter "WCONC" rather than 35,880 mmol/L used as the default value for white matter, which underestimates the absolute metabolite concentrations.<sup>24,25</sup> Based on the LCModel output, MR spectra with line width at full width at half maximum of  $>0.1 \text{ ppm}$  (approximately 6 Hz) and/or SNR of  $<3$  were excluded. Metabolite concentrations with a confidence level of the Cramer-Rao lower bounds<sup>26</sup> of  $>20\%$  were also excluded from the subsequent analysis. LCModel analysis was restricted to fit to the simulated basis spectra of glycerol 3-phosphocholine, phosphocholine, Cr, phosphocreatine, NAA, *N*-acetyl aspartylglutamate, and lactate. Due to the low signal and spectral resolution of TE = 144 milliseconds at 1.5T, the sums of the absolute concentrations total NAA (tNAA) = NAA + *N*-acetyl aspartylglutamate, total Cho (tCho) = glycerol 3-phosphocholine + phosphocholine, total Cr (tCr) = phosphocreatine + Cr, and lactate were used in the analysis because they represent more accurate estimates, as shown from the lower confidence level %SD of the Cramer-Rao lower bounds obtained. The  $-\text{CrCH}_2$  correction term simulated as a negative  $\text{CrCH}_2$  singlet approximately 3.94 ppm was used to correct for attenuation of the  $\text{CrCH}_2$  singlet due to water suppression and differential relaxation effects at the long TE.<sup>27</sup> T1 and T2 relaxation corrections were not applied due to unavailable literature data for the fetal brain between 18 and 40 weeks of pregnancy and because T2 errors in each metabolite have little effect on the metabolite concentrations (approximately 2%).<sup>21</sup> A summary of the quality statistics of the MR spectra acquired is shown in Table 1.

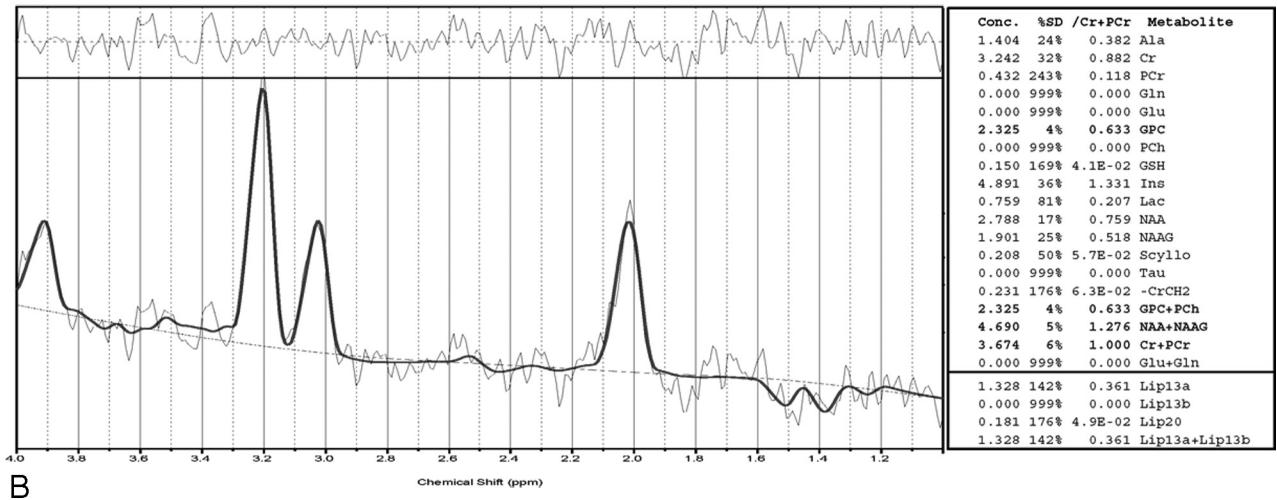
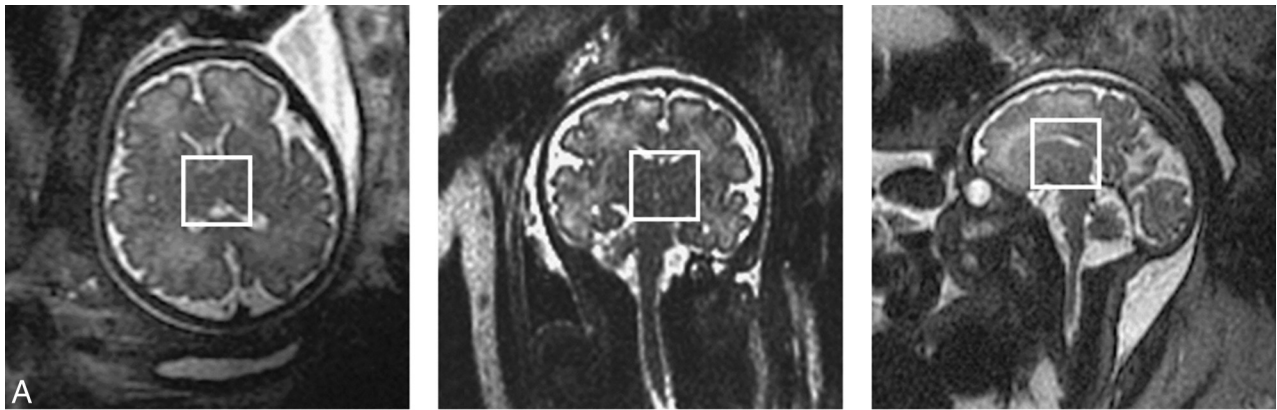


**FIG 1.** A, T2-weighted single-shot fast spin-echo MR imaging (TR/TE = 1100/160 milliseconds, 2-mm thickness) in all 3 orthogonal planes (axial, coronal, and sagittal), showing voxel placement (white rectangle) in a fetus of 35.87 weeks gestation. B,  $^1\text{H}$ -MRS acquired using a point-resolved spectroscopy sequence (TR/TE = 1500/144 milliseconds, voxel  $30 \times 30 \times 30$  mm) quantified using LCMoDel.

**Table 1: Quality statistics of MR spectra acquired: FWHM, SNR, and %SD Cramer-Rao lower bounds in the whole study cohort<sup>a</sup>**

Spectra	FWHM, ppm	SNR	%SD tNAA	%SD tCho	%SD tCr
$n = 153$	$0.07 \pm 0.02$	$7.25 \pm 2.59$	$9.98 \pm 5.51$	$4.80 \pm 1.56$	$10.28 \pm 4.70$

**Note:**—FWHM indicates line width at full width at half maximum.

<sup>a</sup> Values are rounded to 2 decimal places.

### Statistical Analysis

Descriptive statistics, including means, standard deviations, and frequencies were used to characterize the study cohort. Linear regression analysis (least squares method) was used to fit a straight line with 95% confidence intervals (CIs) to the absolute metabolite concentrations and ratios as a function of GA.<sup>28–30</sup> The goodness of fit was assessed using the coefficient of determination ( $r^2$ ) and the standard deviation of the residuals. The slope of the linear regression was tested at  $P < .05$  as indicative of significance. The intraclass correlation coefficient was used to assess scan-rescan measurement reliability within an ANOVA framework. The intraclass correlation coefficient represents concordance and evaluates the level of agreement between raters in measurements, in which 1 is perfect agreement and 0 is no agreement at all.<sup>31</sup> The coefficient of variation, defined as the standard deviation of the mean difference between 2 measurements divided by the mean of all measurements was also used as a measure of dispersion.<sup>32</sup> The coefficient of variation and intraclass correlation coefficient are most commonly used in  $^1\text{H}$ -MRS studies.<sup>33–35</sup> The analysis was

performed using GraphPad Prism 6.05 software (GraphPad Software, San Diego, California). Results are presented as mean (SD) unless otherwise noted.

### RESULTS

A total of 204 MR spectra were acquired from 129 healthy pregnant women during their second and third trimester of pregnancy (mean GA,  $30.63 \pm 6$  weeks). Seventy-one spectra (34.8%) were acquired during the second trimester and 133 (65.2%) during the third trimester. Five subjects' MR spectra (2.45%) were excluded from the analysis due to excessive maternal and fetal movement, lipid contamination, and/or low SNR that precluded any quantification of the metabolite concentrations and metabolite ratios. Three were in the second trimester (mean GA,  $25.43 \pm 1$  week), and 2 were in the third trimester (mean GA,  $34.21 \pm 1$  week). An additional 14 MR spectra of the 204 (6.86%) were also excluded from the analysis at the quantification stage because their metabolite concentrations had a  $>20\%$  confidence level of the Cramer-Rao lower bounds.<sup>26</sup> Twenty-five MR spectra (12.25%) were acquired twice during the examination when time permitted. Of those patients who had 2 MR spectra, the one MR spectrum with higher quality (ie, higher SNR, narrower line width at full width half maximum, and lower %SD of the Cramer-Rao lower bounds) was used in the analysis. An additional 7 randomly se-

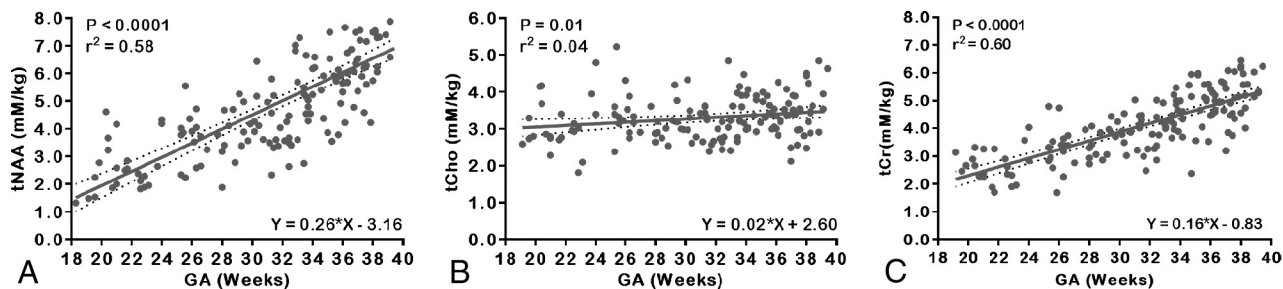


**FIG 2.** Scatterplots of absolute metabolite concentrations relative to the water signal and linear regression straight line fits with mean (solid line) and 95% CIs (dotted lines). A, tNAA. B, tCho. C, tCr.

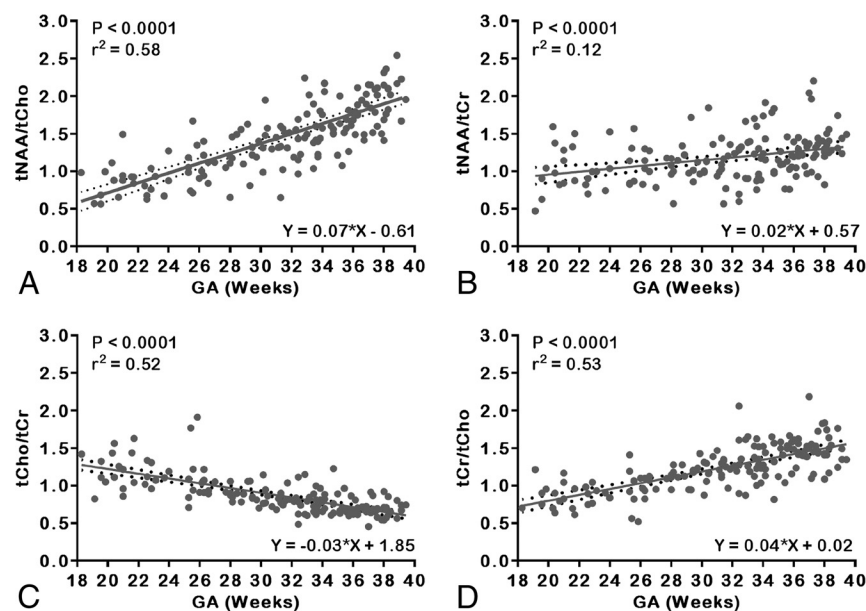


**FIG 3.** Scatterplots of metabolite concentration ratios and linear regression straight line fits with mean (solid line) and 95% CIs (dotted lines). A, tNAA:tCho. B, tNAA:tCr. C, tCho:tCr. D, tCr:tCho.

lected pregnant women had 7 MR spectra (3.43%) acquired (2 in the second trimester and 5 in the third trimester; mean GA,  $31.27 \pm 4$  weeks) that were used for intrasession reproducibility. The remaining 153 MR spectra (75%) (mean GA,  $31.3 \pm 6$  weeks) were included in the final analysis. These included 34 subjects who underwent 2 serial scans, one in the second trimester (mean GA,  $25.6 \pm 5$  weeks) and one in the third trimester (mean GA,  $35.0 \pm 3$  weeks). All the participants' MR images were reviewed by an experienced pediatric neuroradiologist (G.V.) and were found to have structurally normal brains. Postnatal MR studies were performed on 71% of neonates who returned for follow-up MR studies. All the neonates had a structurally normal brain after birth.

### Metabolic Maturation during Second and Third Trimesters

Metabolic profiles in the fetal brain changed significantly with advancing GA. Figure 2 depicts the main absolute metabolite concentrations detected in the fetal brain of the entire cohort across GA, with the best-fit straight line and corresponding 95% CIs. Absolute concentrations of each metabolite using the unsuppressed tissue water as an internal reference and corrected for cerebral water content were also calculated in mM/kg. The tNAA exhibited a significant increase ( $r^2 = 0.58$ ,  $P < .0001$ ) with ad-

vancing GA from 18 to 40 weeks. The tCho increased linearly with GA and was relatively stable across gestation, ( $r^2 = 0.04$ ,  $P = .01$ ) compared with tCr, which increased with GA ( $r^2 = 0.60$ ,  $P < .0001$ ), which made tCho ideal as a denominator for the metabolite ratios.

The tNAA to tCho [tNAA:tCho] also exhibited a significant increase with increasing GA ( $r^2 = 0.58$ ,  $P < .0001$ ), whereas tNAA to tCr [tNAA:tCr] exhibited a slower yet significant increase ( $r^2 = 0.12$ ,  $P < .0001$ ) from 18 to 40 weeks. Similarly, tCho:tCr and tCr:tCho showed a significant exponential increase with GA ( $r^2 = 0.52$ ,  $P < .0001$ ;  $r^2 = 0.53$ ,  $P < .0001$ , respectively). Figure 3 depicts the main metabolite concentration ratios detected in the fetal brain of the entire cohort across GAs, with the best-fit line and corresponding 95% CIs.

Analysis was also performed by stratifying the cohort into 2 groups, that is, those patients who underwent MR studies in the second trimester (43/153 [28%]; mean GA,  $23.62 \pm 2.82$  weeks) versus the third trimester of pregnancy (110/153 [72%]; mean GA,  $34.31 \pm 3$  weeks) to compare metabolic profiles in each trimester alone. In the second trimester group, tCho and tNAA:tCr did not exhibit a significant increase with GA. Conversely tNAA, tNAA:tCho, tCr:tCho, and tCr exhibited a small but significant increase with GA ( $r^2 = 0.17$ ,  $P = .007$ ;  $r^2 = 0.12$ ,  $P = .02$ ;  $r^2 = 0.10$ ,  $P = .034$ ;  $r^2 = 0.20$ ,  $P = .003$ , respectively), whereas tCho:tCr significantly decreased with increasing GA ( $r^2 = 0.23$ ,  $P = .0015$ ). In the third trimester alone, tNAA exhibited the highest increase with GA ( $r^2 = 0.41$ ,  $P < .0001$ ), whereas tNAA:tCr and tCho exhibited a small yet significant increase with GA ( $r^2 = 0.06$ ,  $P = .009$ ). Both tNAA:tCho and tCr exhibited a significant increase with GA ( $r^2 = 0.37$ ,  $P < .0001$ ;  $r^2 = 0.39$ ,  $P < .0001$ , respectively). Similarly, tCr:tCho increased significantly with GA ( $r^2 = 0.20$ ,  $P < .0001$ ), whereas tCho:tCr decreased with GA ( $r^2 = 0.20$ ,  $P < .0001$ ). The normative values for the absolute metabolite concentrations and their corresponding ratios per week of gestation for the study cohort are summarized in Table 2.

In a subset of 21 subjects, 4 in the second trimester (mean GA,  $23.29 \pm 3.5$  weeks) and 17 in the third trimester (mean GA,

**Table 2: Normative mean absolute metabolite concentrations and ratios per GA in weeks for the whole cohort<sup>a</sup>**

	GA, wk										
	18–20	20–22	22–24	24–26	26–28	28–30	30–32	32–34	34–36	36–38	38–40
tNAA, mM/kg	1.87 ± 0.62	3.01 ± 0.91	2.63 ± 0.96	3.76 ± 1.07	3.32 ± 0.78	4.09 ± 0.77	4.27 ± 1.05	4.96 ± 1.44	5.69 ± 1.24	6.52 ± 1.50	7.58 ± 1.27
tCho, mM/kg	2.55 ± 0.72	3.15 ± 0.65	3.12 ± 0.89	3.58 ± 0.85	3.13 ± 0.40	3.16 ± 0.46	3.15 ± 0.52	3.29 ± 0.64	3.43 ± 0.37	3.44 ± 0.75	3.70 ± 0.65
tCr, mM/kg	2.34 ± 0.83	2.59 ± 0.58	2.72 ± 0.71	3.30 ± 1.06	3.21 ± 0.50	3.68 ± 0.52	3.81 ± 0.69	4.28 ± 0.64	4.78 ± 0.96	5.01 ± 0.79	5.37 ± 0.63
tNAA:tCho	0.76 ± 0.21	0.95 ± 0.22	0.85 ± 0.21	1.07 ± 0.32	1.06 ± 0.20	1.31 ± 0.24	1.37 ± 0.30	1.50 ± 0.31	1.66 ± 0.29	1.93 ± 0.43	2.07 ± 0.26
tNAA:tCr	0.89 ± 0.36	1.17 ± 0.28	0.97 ± 0.24	1.25 ± 0.61	1.04 ± 0.22	1.12 ± 0.24	1.14 ± 0.29	1.17 ± 0.32	1.23 ± 0.32	1.32 ± 0.32	1.41 ± 0.15
tCho:tCr	1.14 ± 0.24	1.25 ± 0.26	1.14 ± 0.13	1.17 ± 0.44	0.99 ± 0.11	0.86 ± 0.11	0.84 ± 0.12	0.78 ± 0.16	0.74 ± 0.16	0.69 ± 0.10	0.69 ± 0.09
tCr:tCho	0.91 ± 0.20	0.83 ± 0.18	0.88 ± 0.10	0.95 ± 0.31	1.02 ± 0.10	1.17 ± 0.14	1.21 ± 0.16	1.33 ± 0.27	1.39 ± 0.17	1.49 ± 0.23	1.47 ± 0.19

<sup>a</sup> Values are rounded to 2 decimal places.

**Table 3: Summary of the reproducibility statistics<sup>a</sup>**

Metabolite Concentration	CV, %	ICC (95% CI)
tNAA	6.15	0.90 (0.35–0.97)
tCho	9.30	0.72 (0.62–0.95)
tCr	5.43	0.96 (0.77–0.99)

**Note:**—CV indicates coefficient of variation; ICC, intraclass correlation.

<sup>a</sup> Values are rounded to 2 decimal places.

34.75 ± 2.6 weeks), there was quantifiable lactate in the LCModel fitted spectra with %SD confidence level of Cramer-Rao lower bounds of 16.14 ± 3.1, which was higher than the uncertainty of other metabolite concentrations. Absolute metabolite concentration of lactate was 4.36 ± 2.13 mmol/L/kg, which showed greater variability than the other metabolite concentrations. In all these subjects, none of their postnatal MR studies showed evidence of lactate or any structural brain abnormalities.

### Reproducibility and Repeatability

Seven MR spectra (3.43%) acquired at random from 7 study participants (2 in the second trimester and 5 in the third trimester; mean GA, 31.27 ± 4 weeks) were used in intrasession reproducibility of the results. These were acquired an average of 20 minutes apart to test reproducibility and repeatability of voxel placement and subsequent absolute metabolite concentration quantification. Scan-rescan coefficient of variation was 6.15% for tNAA, 9.30% for tCho, and 5.43% for tCr. Intraclass correlation coefficient was highest for tCr, which showed high concordance with repeated measurements. The reproducibility statistics are shown in Table 3.

## DISCUSSION

In this study, we demonstrated that absolute metabolite concentrations and metabolite ratios using <sup>1</sup>H-MRS can be successfully obtained from the in vivo fetal brain in >75% of cases. In so doing, we provided normative data at TE = 144 milliseconds for metabolic development of the fetal brain over the latter half of gestation in the largest cohort of healthy fetuses to date. We demonstrated that metabolite ratios in the normal fetal brain change with GA as energy demands and cellular maturation increases and cerebral structure evolves. We quantified the detection of the tNAA peak from 18 weeks onward; to our knowledge, this is the earliest detection of tNAA in vivo reported to date. Also to our knowledge, this is the first study to provide absolute metabolite concentrations corrected for water concentration of the fetal brain (cerebrum) and provided clinically relevant values in units of mM/kg. This represents a more accurate estimation of the absolute metabolite concentrations otherwise underestimated if this correction is not used.<sup>25</sup> Inherent limitations with metabolite ra-

tios and misconceptions that they self-correct for type of scanner, localization method differences, gain instabilities, regional susceptibility variations, and partial volume effects are addressed using absolute metabolite concentrations in addition to ratios.<sup>36</sup>

This is also the first study to report intrasession reproducibility and repeatability in fetal <sup>1</sup>H-MRS. Although it is difficult to achieve high reproducibility due to the inherent fetal motion and voxel placement, our results compared favorably with similar studies in the liver<sup>34</sup> and adult brain<sup>33,37</sup> that used similar voxel sizes to acquire MR spectra.

Very few studies have explored fetal brain <sup>1</sup>H-MRS in vivo. Most of these studies reported metabolite peak ratios or metabolite areas that are very different and might not be clinically significant from the absolute metabolite concentrations or ratios that LCModel quantifies. Heerchap and van den Berg<sup>12</sup> first performed a feasibility study of 6 healthy third-trimester fetuses using long acquisition times (>10 minutes). Fenton et al<sup>38</sup> reported metabolites in a small sample using a short breath-hold technique, but spectral quality remained poor. Subsequently, Kok et al<sup>39</sup> studied 36 normal third trimester fetuses and described a significant increase in both NAA:Cr and NAA:Cho, whereas Cho:Cr decreased with increasing GA. Using maternal sedation, Girard et al<sup>28</sup> performed clinically indicated studies in 58 fetuses in which fetal MR imaging studies were found to be structurally normal. However, they reported ratios of each metabolite to the total metabolite sum, which makes these data difficult to compare with other studies. Also, their long acquisition times (twice as long as our study) and their voxel placement in the centrum semiovale was different enough from ours to be able to make any meaningful comparisons. Most recently, Berger-Kulemann et al<sup>40</sup> retrospectively evaluated, with a 55% success rate, <sup>1</sup>H-MRS of 75 fetuses referred for MR imaging for suspected brain abnormalities.<sup>41</sup> It is important to note that, unlike other studies, our inception cohort only included low-risk healthy pregnant volunteers, which constituted a truly representative normative sample. We also demonstrated a higher success in interpretable <sup>1</sup>H-MRS in the absence of maternal sedation.

The increase in both tNAA:tCho and tNAA:tCr with advancing GA described in our study may be attributed to dendritic and synaptic development.<sup>5</sup> The tCho peak observed in our MR spectra was composed of both phosphocholine and glycerol 3-phosphocholine. These compounds are involved in membrane synthesis and degradation.<sup>7</sup> This tCho peak, however, only reflects a small part of the tissue level of Cho-containing compounds. More than 90% of the latter is phosphatidylcholine, a major constituent of the phospholipids that form myelin,<sup>42,43</sup> which cannot be detected by <sup>1</sup>H-MRS.<sup>44</sup> The tCho exhibits a higher concentration

during early life than in adulthood, which indicates that Cho-containing compounds are turned over more rapidly during early human development<sup>24,45</sup> and decrease over the first 5 years of life.<sup>46,47</sup> We also showed that tCho:tCr decreases with increasing GA, whereas tCho remains relatively stable until the beginning of myelination toward the end of the third trimester of pregnancy and early postnatal period.<sup>45,48</sup> One study reported that absolute Cr levels remain stable during gestation, which may serve as a reliable reference (denominator) for quantifying changes in other metabolites.<sup>29</sup> Analysis of our data indicated that tCho may be a more appropriate reference metabolite for the developing fetal brain because it remains at relatively constant levels from 18 to 40 weeks of gestation, as shown by the tCho linear regression straight line plot and shown from the absolute metabolite concentrations quantified using the unsuppressed tissue water as an internal reference<sup>20</sup> in Table 2. However, there is a small increase in tCho when considering the cohort in the third trimester alone, which likely indicated the start of myelination.

Lactate was observed in a small subset of our cohort. Berger-Kulemann et al<sup>40</sup> found lactate in 2 of their 6 normal fetuses (33.3%), whereas Story et al<sup>30</sup> described lactate in 3 healthy fetuses (7%) with normal deliveries and postnatal outcomes. The investigators postulate that lactate may be an important source of energy for the normally developing brain. Lactate is also normally present in CSF.<sup>49</sup> The voxel used in this study contained heterogeneous brain tissue, including contamination by CSF, which led to the detection of lactate signal. Because our choice of TE (144 milliseconds) is specific to lactate, it is likely more frequently detected when present. Furthermore, the absolute metabolite concentration of lactate exhibited a greater variability than any of the other metabolites, which indicated that the fluctuating baseline might also be responsible for its detection. No lactate peak was identified in the postnatal <sup>1</sup>H-MRS. Further studies are needed to investigate the presence and predictive value of lactate in the healthy fetus.

The choice of TE often depends on the metabolite of interest. In this study, we chose TE = 144 milliseconds because this has a better-defined baseline and less baseline distortion over TE = 35 milliseconds, which allowed for a more accurate quantification as indicated by lower %SD of the Cramer-Rao lower bounds. In addition, our normative fetal <sup>1</sup>H-MRS studies were performed to be able to compare brain metabolites in a cohort of fetuses with complex congenital heart disease, in which we selected TE = 144 milliseconds to detect and differentiate lactate from lipids at 1.3 to 1.4 ppm by J-modulation/inversion of the lactate doublet peaks.

Strengths of our study included the largest known sample size of healthy normal fetal studies, the prospective design, and the successful acquisition and correction of motion-induced artifacts, which yielded high-quality spectra in >75% of the studies. Limitations included the fact that single voxel fetal brain <sup>1</sup>H-MRS requires an additional anatomic scan for voxel placement and is usually relatively large to increase SNR. This is needed given the magnitude and frequency of fetal-maternal motion to ensure that it remains within the brain. However, the voxel usually contains white-gray matter and CSF.<sup>15</sup> To overcome this limitation would require tissue segmentation to resolve tissue constituents from

which the MR spectrum is acquired, which is currently not possible in utero.<sup>39</sup>

This study demonstrated the feasibility of obtaining noninvasive metabolic information from the fetal brain with a high success rate and good reproducibility using <sup>1</sup>H-MRS. Normative reference values of absolute metabolite concentrations and ratios in the fetal brain in the second and third trimesters of pregnancy are provided for the largest sample to date. This is also the first study to retrospectively correct the acquired MR spectra for motion-induced artifacts before quantification, which yielded high-quality spectra. These data will aid clinicians in interpreting <sup>1</sup>H-MRS of the fetal brain, complementing structural MR imaging, and allowing detection of early deviation from these norms in the compromised fetus. In the future, detection of such deviation from normal metabolic development may allow interventions that minimize irreversible brain injury.

## ACKNOWLEDGMENTS

The authors thank the clinical research coordinators, the MR technologists, and the volunteers and their families for participating in this study.

Disclosures: Iordanis Evangelou—RELATED: Grant: Canadian Institutes of Health Research (MOP-81116)\*; UNRELATED: Board Membership: ImPossible MR, LLC; Consultancy: GE Healthcare Coils, MR Instruments; Employment: ImPossible MR, LLC; Grants/Grants Pending: Veterans Affairs, Department of Defense,\* Chronic Effects of Neurotrauma Consortium (CENC0039P); Stock/Stock Options: ImPossible MR, LLC. Ralph Noeske—UNRELATED: Employment: GE Healthcare. \*Money paid to the institution.

## REFERENCES

1. Fayed N, Morales H, Modrego PJ, et al. **White matter proton MR spectroscopy in children with isolated developmental delay: does it mean delayed myelination?** *Acad Radiol* 2006;13:229–35 CrossRef Medline
2. Broom KA, Anthony DC, Lowe JP, et al. **MRI and MRS alterations in the preclinical phase of murine prion disease: association with neuropathological and behavioural changes.** *Neurobiol Dis* 2007;26:707–17 CrossRef Medline
3. Barker PB. **N-acetyl aspartate—a neuronal marker?** *Ann Neurol* 2001;49:423–24 CrossRef Medline
4. Moffett JR, Ross B, Arun P, et al. **N-Acetylaspartate in the CNS: from neurodiagnostics to neurobiology.** *Prog Neurobiol* 2007;81:89–131 CrossRef Medline
5. Urenjak J, Williams SR, Gadian DG, et al. **Specific expression of N-acetylaspartate in neurons, oligodendrocyte-type-2 astrocyte progenitors, and immature oligodendrocytes in vitro.** *J Neurochem* 1992;59:55–61 CrossRef Medline
6. Sartorius A, Lugenbiel P, Mahlstedt MM, et al. **Proton magnetic resonance spectroscopic creatine correlates with creatine transporter protein density in rat brain.** *J Neurosci Methods* 2008;172:215–19 CrossRef Medline
7. Gill SS, Small RK, Thomas DG, et al. **Brain metabolites as <sup>1</sup>H NMR markers of neuronal and glial disorders.** *NMR Biomed* 1989;2:196–200 CrossRef Medline
8. Katz-Brull R, Koudinov AR, Degani H. **Choline in the aging brain.** *Brain Res* 2002;951:158–65 CrossRef Medline
9. José da Rocha A, Túlio Braga F, Carlos Martins Maia A Jr, et al. **Lactate detection by MRS in mitochondrial encephalopathy: optimization of technical parameters.** *J Neuroimaging* 2008;18:1–8 CrossRef Medline
10. Wolffberg AJ, Robinson JN, Mulkern R, et al. **Identification of fetal cerebral lactate using magnetic resonance spectroscopy.** *Am J Obstet Gynecol* 2007;196:e9–e11 CrossRef Medline

11. Charles-Edwards GD, Jan W, To M, et al. **Non-invasive detection and quantification of human foetal brain lactate in utero by magnetic resonance spectroscopy.** *Prenat Diagn* 2010;30:260–66 CrossRef Medline
12. Heerschap A, van den Berg PP. **Proton magnetic resonance spectroscopy of human fetal brain.** *Am J Obstet Gynecol* 1994;170:1150–51 CrossRef Medline
13. Brighina E, Bresolin N, Pardi G, et al. **Human fetal brain chemistry as detected by proton magnetic resonance spectroscopy.** *Pediatr Neurol* 2009;40:327–42 CrossRef Medline
14. Pugash D, Krssak M, Kulemann V, et al. **Magnetic resonance spectroscopy of the fetal brain.** *Prenat Diagn* 2009;29:434–41 CrossRef Medline
15. Story L, Damodaram MS, Allsop JM, et al. **Proton magnetic resonance spectroscopy in the fetus.** *Eur J Obstet Gynecol Reprod Biol* 2011;158:3–8 CrossRef Medline
16. Limperopoulos C, Towitzky W, McElhinney DB, et al. **Brain volume and metabolism in fetuses with congenital heart disease: evaluation with quantitative magnetic resonance imaging and spectroscopy.** *Circulation* 2010;121:26–33 CrossRef Medline
17. Clouchoux C, Guizard N, Evans AC, et al. **Normative fetal brain growth by quantitative in vivo magnetic resonance imaging.** *Am J Obstet Gynecol* 2012;206:173.e1–8 CrossRef Medline
18. Evangelou IE, Noeske R, Limperopoulos C. **Retrospective correction of motion induced artifacts in 1H magnetic resonance spectroscopy of the fetal brain.** In: *Proceedings of the IEEE 12th International Symposium on Biomedical Imaging*, Brooklyn, New York. April 16–19, 2015:853–57
19. Provencher SW. **Estimation of metabolite concentrations from localized in vivo proton NMR spectra.** *Magn Reson Med* 1993;30:672–79 CrossRef Medline
20. Longo R, Bampo A, Vidimari R, et al. **Absolute quantitation of brain 1H nuclear magnetic resonance spectra. Comparison of different approaches.** *Invest Radiol* 1995;30:119–203 CrossRef Medline
21. Kreis R, Ernst T, Ross BD. **Development of the human brain: in vivo quantification of metabolite and water content with proton magnetic resonance spectroscopy.** *Magn Reson Med* 1993;30:424–37 CrossRef Medline
22. Diem K, Lentner C. *Scientific Tables*. Basle: J.R. Geigy; 1970
23. Ganguly A. *Fundamentals of Physical Chemistry*. New Delhi: Pearson Education India; 2012
24. Kreis R, Hofmann L, Kuhlmann B, et al. **Brain metabolite composition during early human brain development as measured by quantitative in vivo 1H magnetic resonance spectroscopy.** *Magn Reson Med* 2002;48:949–58 CrossRef Medline
25. Tomiyasu M, Aida N, Endo M, et al. **Neonatal brain metabolite concentrations: an in vivo magnetic resonance spectroscopy study with a clinical MR system at 3 Tesla.** *PloS One* 2013;8:e82746 CrossRef Medline
26. Cavassila S, Deval S, Huegen C, et al. **Cramér-Rao bounds: an evaluation tool for quantitation.** *NMR Biomed* 2001;14:278–83 CrossRef Medline
27. Provencher SW. **Automatic quantitation of localized in vivo 1H spectra with LCModel.** *NMR Biomed* 2001;14:260–64 CrossRef Medline
28. Girard N, Gouny SC, Viola A, et al. **Assessment of normal fetal brain maturation in utero by proton magnetic resonance spectroscopy.** *Magn Reson Med* 2006;56:768–75 CrossRef Medline
29. Kok RD, van den Berg PP, van den Bergh AJ, et al. **Maturation of the human fetal brain as observed by 1H MR spectroscopy.** *Magn Reson Med* 2002;48:611–16 CrossRef Medline
30. Story L, Damodaram MS, Allsop JM, et al. **Brain metabolism in fetal intrauterine growth restriction: a proton magnetic resonance spectroscopy study.** *Am J Obstet Gynecol* 2011;205:483.e1–8 CrossRef Medline
31. Stanish WM, Taylor N. **Estimation of the intraclass correlation coefficient for the analysis of covariance model.** *Am Stat* 1983;37:221–24 CrossRef
32. Kirkwood TB. **Geometric means and measures of dispersion.** *Biometrics* 1979;35:908–09
33. Marshall I, Wardlaw J, Cannon J, et al. **Reproducibility of metabolite peak areas in 1H MRS of brain.** *Magn Reson Imaging* 1996;14:281–92 CrossRef Medline
34. van Werven JR, Hoogduin JM, Nederveen AJ, et al. **Reproducibility of 3.0 Tesla magnetic resonance spectroscopy for measuring hepatic fat content.** *J Magn Reson Imaging* 2009;30:444–48 CrossRef Medline
35. Gasparovic C, Bedrick EJ, Mayer AR, et al. **Test-retest reliability and reproducibility of short-echo-time spectroscopic imaging of human brain at 3T.** *Magn Reson Med* 2011;66:324–32 CrossRef Medline
36. Li BS, Wang H, Gonen O. **Metabolite ratios to assumed stable creatine level may confound the quantification of proton brain MR spectroscopy.** *Magn Reson Imaging* 2003;21:923–28 CrossRef Medline
37. Wijtenburg SA, Rowland LM, Edden RA, et al. **Reproducibility of brain spectroscopy at 7T using conventional localization and spectral editing techniques.** *J Magn Reson Imaging* 2013;38:460–67 CrossRef Medline
38. Fenton BW, Lin CS, Macedonia C, et al. **The fetus at term: in utero volume-selected proton MR spectroscopy with a breath-hold technique—a feasibility study.** *Radiology* 2001;219:563–66 CrossRef Medline
39. Kok RD, van den Bergh AJ, Heerschap A, et al. **Metabolic information from the human fetal brain obtained with proton magnetic resonance spectroscopy.** *Am J Obstet Gynecol* 2001;185:1011–15 CrossRef Medline
40. Berger-Kulemann V, Brugger PC, Pugash D, et al. **MR spectroscopy of the fetal brain: is it possible without sedation?** *AJNR Am J Neuroradiol* 2013;34:424–31 CrossRef Medline
41. Brunel H, Girard N, Confort-Gouny S, et al. **Fetal brain injury.** *J Neuroradiol* 2004;31:123–37 CrossRef Medline
42. Smith ME. **A regional survey of myelin development: some compositional and metabolic aspects.** *J Lipid Res* 1973;14:541–51 Medline
43. Podbielska M, Banik NL, Kurowska E, et al. **Myelin recovery in multiple sclerosis: the challenge of remyelination.** *Brain Sci* 2013;3:1282–324 CrossRef Medline
44. Miller BL, Chang L, Booth R, et al. **In vivo 1H MRS choline: correlation with in vitro chemistry/histology.** *Life Sci* 1996;58:1929–35 CrossRef Medline
45. Hüppi PS, Posse S, Lazeyras F, et al. **Magnetic resonance in preterm and term newborns: 1H-spectroscopy in developing human brain.** *Pediatr Res* 1991;30:574–78 CrossRef Medline
46. Danielsen ER, Ross B. *Magnetic Resonance Spectroscopy Diagnosis of Neurological Diseases*. New York: M. Dekker; 1999
47. Pouwels PJ, Brockmann K, Kruse B, et al. **Regional age dependence of human brain metabolites from infancy to adulthood as detected by quantitative localized proton MRS.** *Pediatr Res* 1999;46:474–85 CrossRef Medline
48. Holland BA, Haas DK, Norman D, et al. **MRI of normal brain maturation.** *AJNR Am J Neuroradiol* 1986;7:201–08 Medline
49. Nagae-Poetscher LM, McMahon M, Braverman N, et al. **Metabolites in ventricular cerebrospinal fluid detected by proton magnetic resonance spectroscopic imaging.** *J Magn Reson Imaging* 2004;20:496–500 CrossRef Medline